TOPOGRAPHIC ASSESSMENT OF HOLLOWS ON MERCURY: DISTINGUISHING AMONG FORMATION HYPOTHESES. L.R. Ostrach[1] and C.M. Dundas[1], [1]U.S. Geological Survey, Astrogeology Science Center, 2255 N. Gemini Dr., Flagstaff, AZ 86001. (correspondence: lostrach@usgs.gov)

Introduction: The discovery of hollows on Mercury remains one of the most surprising scientific findings by MESSENGER. Hollows are sharp-edged, irregular, rimless pits that are often surrounded by bright haloes [1] and form primarily in terrains exhibiting reflectance values lower than that of the global average [e.g., 2–5]. Hollows are interpreted to represent volatile-loss landforms on the basis of geomorphic and remotely sensed geochemical observations [e.g., 1,2,4,6–10].

The volatile and process(es) responsible for and controlling hollow formation remain unresolved. Multiple hypotheses for hollow formation have been proposed, including (and not limited to) insolation-driven sublimation of volatiles from surface materials, volatile separation and segregation to the top layer of impact melts or extruded lavas, formation of a condensate deposit covered by a protective lag, and exhumation of volatile-rich materials from depth via impact crater formation [e.g., 1,2,4,11,12]. Morphologic observations of hollows suggest that hollow formation may not be controlled by a single process [e.g., 2,4]

Observations of topography, specifically the relationships of hollows to their surroundings, can be used to investigate hollow formation. We will assess the topography of hollows to distinguish among formation hypotheses summarized by Blewett et al. [1,2].

Data and Methods: Mercury Dual Imaging System Narrow Angle Camera (MDIS NAC) stereo images with ≤50 m pixel scales were used to create Digital Terrain Models (DTMs) for analysis at selected hollows sites. These DTMs are used to determine whether hollow-hosting material is ponded, draped, or has some other relation to observed topography. When possible, the thickness and variation in hollow-hosting material is examined and an estimate of volume lost from hollows is calculated for a first-order estimate of the bulk volume of initial hollow-forming material.

Formation Hypotheses Tested with Topography

(1) Ponded materials. If hollows are related to impact-generated melt or extrusive volcanic materials, then the ponded material should closely conform to an equipotential surface. In this case, the un-eroded surface between hollows should be close to level.

(2) Draped materials. If a fall-out or condensate deposit (initially covered by a protective lag) provided the source for hollow formation, the host material should smoothly drape underlying topography with a near-uniform thickness.

(3) Exhumed materials. If exhumation or exposure of volatile-rich materials provides the source materials for hollows, then exhumed/exposed materials within (and surrounding) craters should host hollows. In this case, hollows would be expected in central peaks/peak ring structures, in portions of the crater wall and/or rim, and within the crater floor deposits (some of which may also contain impact melt), and their flat floors would suggest formation of a stabilizing lag deposit.

Preliminary results at Raditladi basin: Raditladi basin [**Fig. 1**] is interpreted to be a young impact basin on the basis of morphology [13,14] and its peak-ring hosts well-developed hollows [1,2]. Described in some detail by Blewett et al. [2], the hollows hosted in the peak-ring of Raditladi basin are numerous and exhibit typical crisp, sharp boundaries and bright haloes.

Of particular interest are the hollows that formed in the northeast portion of the peak-ring, which coalesced along the ridge and have the appearance of being flat-floored [2; **Figs. 2-4**]. Here, the formation of hollows substantially modified the original peak-ring morphology; very little unmodified peak-ring ridge material remains. At ~15 meters per pixel (mpp) the floors of the hollows appear smooth, with exception of the largest hollow that displays a rougher, more dissected texture near the southeast and western margins [**Fig. 3**]. Topographic profiles [**Fig. 4**] for the largest hollow in this area indicate that the hollow floors are relatively flat and controlled in part by surrounding peak-ring topography (e.g., the central mound that may represent a cap or lag deposit).

Colluvium surrounds the base of the peak-ring structure to form an apron, most noticeable on the south-facing slope. There are numerous alcoves that may serve as source regions for this material upslope [**Fig. 5**]. Many of these alcoves are surrounded by bright haloes and initiate from a larger, coalesced hollow, although this relationship is not observed at all the alcoves. It is therefore possible that a combination of continued hollow formation and growth from the peak-ring ridge coupled with mass-wasting resulting from slope retreat could be responsible for apron development.

In summary, larger-scale topographic relationships between hollows and peak-ring material reveal that most hollows in Raditladi are limited to the peak-ring, which supports exhumation as a primary formation mechanism. However, hollows on the crater floor proximal to the peak-ring make it difficult to completely rule out hollow formation from draped materials, since draped materials would not be expected to be of such limited spatial extent and correlated to the ring. Alternatively, it is possible that crater floor hollows formed within mass-wasted materials from the peak-ring.

Acknowledgements: This work was funded by PGG grant NNH14AX97I. We thank Donna Galuszka and Bonnie Redding for producing the MDIS DTMs.

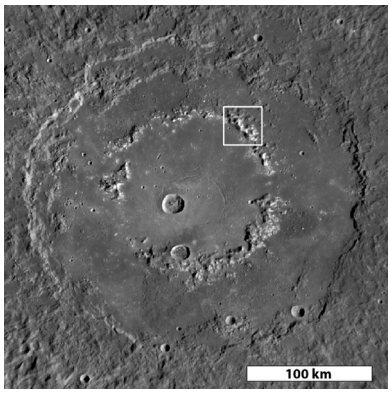

Fig. 1. Context view of Raditladi basin (258 km diameter; 27.15°N, 119.06°E), where some of the most impressive hollows on Mercury formed in peak-ring material. White box is location of MDIS NAC images in Fig. 2; North is up.

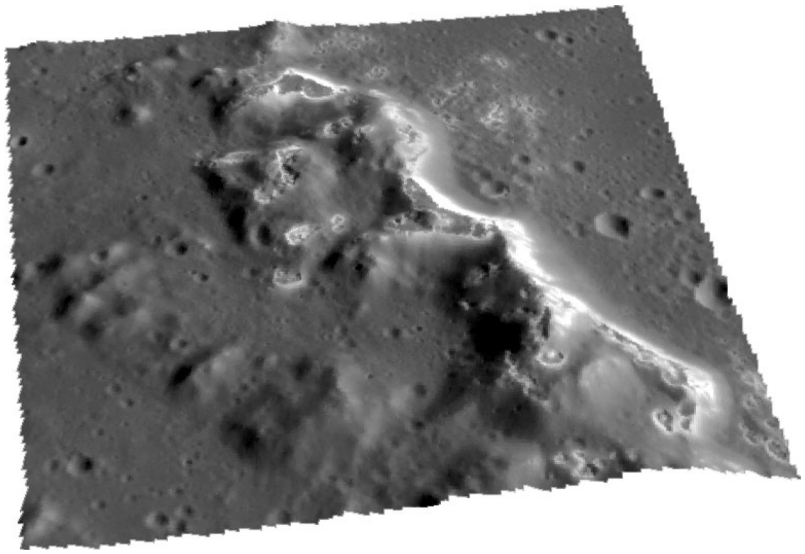

Fig. 2. Perspective view of Raditladi NE peak-ring hollows. Hollows coalesced in this location to form relatively flat-topped areas along peak-ring ridges. A debris apron surrounds much of the NE peak-ring (prominent on the south-facing slope below high-reflectance material, image right), which likely originated as a by-product of hollow formation [Fig. 5]. Peak-ring segment ~25 km across; North is ~down. EN1015454462M (40 mpp) draped over DTM (120 mpp); no vertical exaggeration.

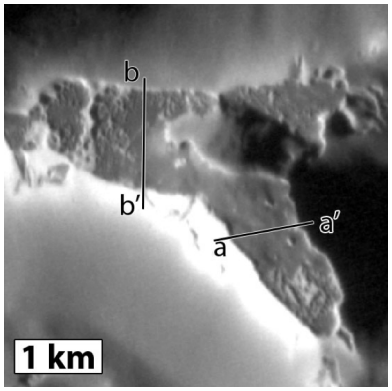

Fig. 3. The floor of this hollow appears smooth and generally flat-floored, surrounding a mound of material in the center. Dissected, rougher textures are observed toward the SE and W edges. EN0221023170M (15 mpp), North is up. Topographic profiles shown in Fig. 4.

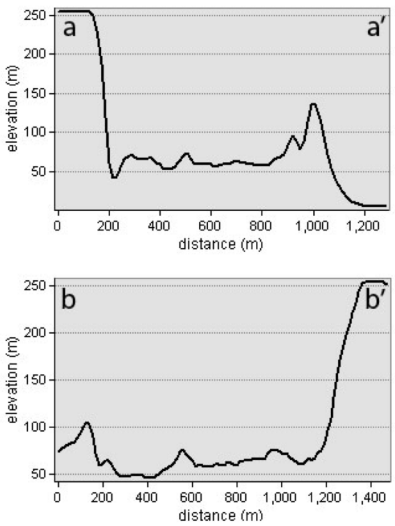

Fig. 4. Some areas of the largest hollow have relatively flat floors; other areas exhibit gentle slopes due to local topography (e.g., near the central mound) and/or larger-scale topography of the peak-ring materials. The topography of smaller hollows is less well-resolved, but their topography can be investigated with respect to interactions with larger-scale features. Topography from 120 mpp DTM.

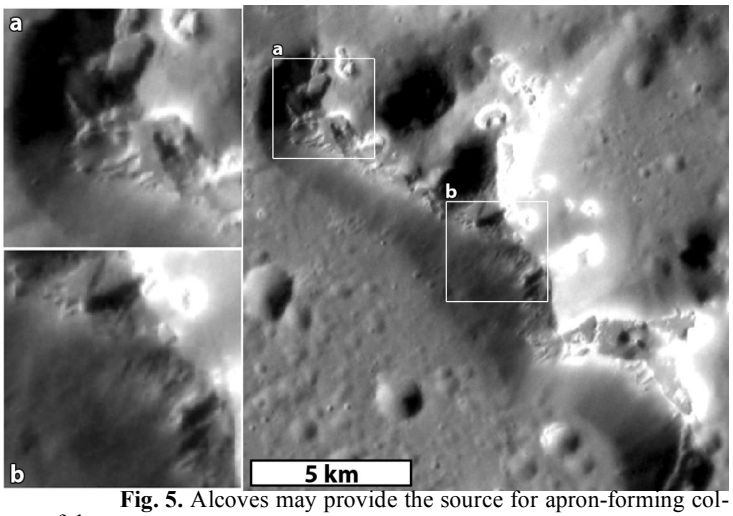

Fig. 5. Alcoves may provide the source for apron-forming colluvium. (a), (b) are zoomed-in views of two notable locations; (b) in particular exhibits morphology indicative of hollow formation progressing from the peak-ring ridge downslope. Most alcoves originate from within hollows that formed along the peak-ring ridge and are surrounded by bright haloes [Fig. 2], suggesting that hollow formation may be ongoing in these materials. EN1025853410M (35 mpp), North is up.

References: [1] Blewett D.T. et al. (2011) *Science*, *333*, 1856–1859. [2] Blewett D.T. et al. (2013) *JGR Planets*, *118*, 1013–1032. [3] Xiao Z. et al. (2013) *JGR Planets*, *118*, 1752–1765. [4] Thomas R.J. et al. (2014) *Icarus*, *229*, 221–235. [5] Denevi B.W. et al. (2009) *Science*, *324*, 613–618. [6] Nittler L.R. et al. (2011) *Science*, *333*, 1847–1850. [7] Weider S.Z. et al. (2015) *EPSL*, *416*, 109–120. [8] Peplowski P.N. et al. (2012) *JGR Planets*, *117*, E00L04. [9] Peplowski P.N. et al. (2014) *Icarus*, *228*, 86–95. [10] Peplowski P.N. et al. (2016) *Nat. Geosci.*, *9*, 273–276. [11] Vaughan W.M. et al. (2012) *LPS*, *43*, Abst. 1187. [12] Helbert J. et al. (2013) *EPSL*, *369–370*, 233–238. [13] Strom et al. (2008) *Science*, *321*, 79–81. [14] Prockter et al. (2010) *Science*, *329*, 668–671.